CHAOS
Theory and Applications
in Applied Sciences and Engineering

e-ISSN: 2687-4539
RESEARCH ARTICLE
Vol.2 / No.2 / 2020 / pp.77-89

Multistability and its Annihilation in the Chua's Oscillator with Piecewise-Linear Nonlinearity

Zeric Tabekoueng Njitacke [*,†,1], **Théophile Fonzin Fozin** [‡,2], **Léandre Kengne Kamdjeu** [†,§,3], **Gervais Dolvis Leutcho** [δ,4], **Edwige Mache Kengne** [§,5] **and Jacques Kengne** [†,6]

[*]Department of Electrical and Electronic Engineering, College of Technology (COT), University of Buea, Buea 63, Cameroon, [‡]Department of Electrical and Electronic Engineering, Faculty of Engineering and Technology (FET), University of Buea, Buea 63, Cameroon, [†]Unité de Recherche d'Automatique et Informatique Appliquée (LAIA), Department of Electrical Engineering, IUT-FV Bandjoun, University of Dschang, Cameroon, [§]Unité de Recherche de Matière Condensée, d'Electronique et de Traitement du Signal (LAMACETS), Department of Physics, University of Dschang. P.O. Box 67, Dschang, Cameroon, [δ]Department of Physics, Faculty of Sciences, University of Mons, P.O. Box 7000, Mons, Belgium.

ABSTRACT This contribution uncovers numerical evidence of hysteric dynamical behaviors for the same set of the circuit parameters of the Chua's circuit with traditional piecewise-linear nonlinearity. Stationary points and the symmetry property of the model first forecast the possible evidence of coexisting attractors. Then, well known nonlinear analysis approach based on the bifurcation diagrams, two-parameter diagrams, phase portraits, two parameter Lyapunov exponent diagrams, graph of maximum Lyapunov exponents, and attraction basins are exploited to characterize the dynamical behavior of the oscillator including coexisting orbits. Finally, the simultaneous existence of both periodic and chaotic orbits highlighted in the Chua's oscillator is also annihilated based on linear controller. Numerical findings indicate control method 's efficacy by combining two periodic routes and one chaotic route with another chaotic route.

KEYWORDS
Chaotic systems
Chua's oscillator
Piecewise-linear nonlinearity
Multistability control
Merging crisis.

INTRODUCTION

Chua's circuit, which is the famous chaos generator is an ideal paradigm for nonlinear phenomena study, has been investigated intensively during the last years Chua *et al.* (1986); Chua (1994, 1998); Duan *et al.* (2007); Huang *et al.* (1996); Kengne (2017). In the traditional Chua's circuit, the nonlinear element responsible of complex behavior found in the circuit is designed using a piecewise linear (PWL) function (Chua's diode) Matsumoto (1984); Ramírez-Ávila and Gallas (2010); Zhong and Ayrom (1985).

It is well known that, the piecewise linear nonlinearity enables solely the first-order description of the real Chua's circuit Kengne *et al.* (2016). This is why smooth nonlinearity is suitable from a computational point of view since it is used for a better characterization of both the irregular and regular behaviors of the oscillator. The current-voltage characteristics of the nonlinear components in real circuits are generally smooth curves hence; Chua's equation with a smooth (cubic) nonlinearity was established Hartley (1989).

Chua's equations with smooth nonlinearity have been extensively studied and plethora of nonlinear behavior found with the PWL function were also found with the smooth (cubic) nonlinearity Tsuneda (2005); Ramírez-Ávila and Gallas (2010). Among phenomena found in Chua's circuit, we have period-doubling bifurcations, period-adding bifurcation, intermittency bifurcations, torus breakdown route to chaos, bubble bifurcation, hidden attractors as well as coexisting attractors Leonov *et al.* (2011); Zhong (1994); Huang *et al.* (1996); Chua (1994). This latter phenomenon also known as simultaneous existence of multiple orbits/attractors is a widespread in the variants of Chua's oscillator Bao *et al.* (2016, 2015a,b); Chen *et al.* (2015); Xu *et al.* (2016).

The extreme / hidden extreme multi-stability observed

Manuscript received: 7 July 2020,
Revised: 13 September 2020,
Accepted: 15 September 2020.

[1] zerictabekoueng@yahoo.fr (**Corresponding Author**)
[2] fozintheo@gmail.com
[3] kamdjeukengneleandre@yahoo.fr
[4] leutchoeinstein@yahoo.com
[5] edwigemache7@gmail.com
[6] kengnemozart@yahoo.fr

in the memristor-based Chua circuit is regarded as a strange and striking manifestation of this phenomenon. Out of Kengne (2017) who present coexistence of up to four disconnected attractor in Chua's equation with a cubic nonlinearity, there is no work in the literature focused on the discovery of this phenomenon in the original Chua's equation with piecewise linear nonlinearity. In addition such nonlinear phenomenon as well as their circuit implementation have already been found in several others classes of nonlinear dynamical systems Adiyaman *et al.* (2020); Kingni *et al.* (2020); Tuna *et al.* (2019).

It is good to mention that, the smooth (cubic) nonlinearity is only an approximation of the nonlinear element of the Chua's circuit due to the fact in experimental realization the $(v-i)$ characteristic of the Chua's diode also known as nonlinear resistor is smooth Tsuneda (2005); Zhong (1994). Then, it is important to prove that the original Chua's equation is also able to exhibit coexistence of up to four disconnected attractor in order to support the fact that the model with smooth nonlinearity is able reproduce all the dynamics of the one with PWL nonlinearity. To achieve this objective, the dynamics of the original Chua's equation is numerically investigated in this contribution.

The remainder of this contribution is organized as follows. Section 2 is focused on the modeling process. Some basic features of the mathematical model including symmetry property as well as the stability of the rest points are underlined. Section 3 focuses on the numerical analysis. Various nonlinear diagnostic tools are used to track the windows in which the Chua's model with piecewise-linear function exhibits hysteretic dynamics. Section 4 is devoted to the multistability control in the Chua's circuit using linear augmentation scheme. Finally, in the conclusion part, some proposals for future works are given in Section 5.

PRESENTATION OF THE CHUA'S OSCILLATOR BASED ON ITS ORIGINAL NONLINEARITY

Mathematical model of the oscillator

Attractors of the Chua circuit depicted in Fig1 have been firstly found by computer simulations in Zhong and Ayrom (1985). In the same line, its experimental validation has been carried out by Ramírez-Ávila and Gallas (2010). Chua's oscillator can be viewed as the most studied nonlinear circuit capable to generate complex bifurcations and chaotic phenomena. That circuit is built using two capacitors (C1, C2), two resistors (R0, R), one inductor L and a nonlinear resistor N_R. This nonlinear resistor which is at the origin of all complex phenomena found is called Chua's diode.

The set of equations describing the model is given by Tsuneda (2005) for model C-12.

$$\begin{cases} \frac{dv_1}{dt} = \frac{1}{C_1}\left[G\left(v_2 - v_1\right) - f\left(v_1\right)\right] \\ \frac{dv_2}{dt} = \frac{1}{C_2}\left[G\left(v_2 - v_1\right) + i_L\right] \\ \frac{di_L}{dt} = \frac{1}{L}\left(v_2 + R_0 i_L\right) \end{cases} \tag{1}$$

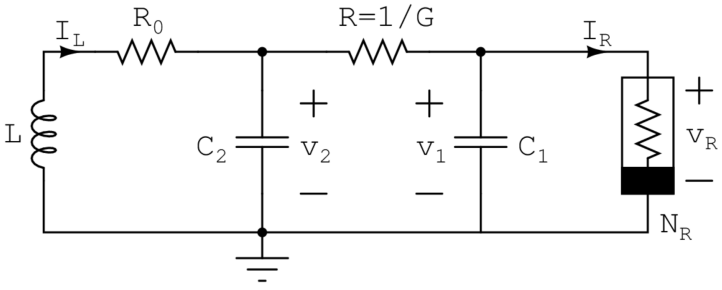

Figure 1 Schematic diagram of Chua's oscillator.

Where $f\left(.\right)$ is the current-voltage characteristic $(v-i)$ of the nonlinear element N_R (Chua's diode).

$$f\left(v_1\right) = G_b v_1 + \frac{1}{2}\left(G_a - G_b\right)\left\{\left|v_1 + E\right| - \left|v_1 - E\right|\right\} \tag{2}$$

With the following change of variables and parameters

$$x_1 = \frac{v_1}{E}, x_2 = \frac{v_2}{E}, x_3 = i_3\frac{R}{E}, \alpha = \frac{C_2}{C_1}, \beta = \frac{R^2 C_2}{L}\gamma = \frac{RR_0C_2}{L}, \tag{3}$$

$m_0 = RG_a, m_1 = RG_b, k = 1 if RC_2 > 0, k = -1 if RC_2 < 0.$

where G_a and G_b represent the conductance slopes of the inner and E stand for the voltage breakpoint. From Eq.(3) it is observed that $k = 1$ if $RC_2 > 0$, $k = -1$ if $RC_2 < 0$. The practical conditions to have the negative product of resistance and capacity ($k = -1$ if $RC_2 < 0$) is to replace the dissipative resistor in the case $k = 1$ by a negative resistor which is an active device and enables to bring the energy to the Chua's circuit. This is the concept that the authors wanted to highlight in their work Zhong and Ayrom (1985).

The dimensionless expression of the Chua's model is given by:

$$\begin{cases} \frac{dx_1}{dt} = k\alpha\left(x_2 - x_1 - f\left(x_1\right)\right) \\ \frac{dx_2}{dt} = k\left(x_1 - x_2 + x_3\right) \\ \frac{dx_3}{dt} = k\left(-\beta x_2 - \gamma x_3\right) \end{cases} \tag{4}$$

From (4) the nonlinear term $f\left(.\right)$ is given by

$$f(x) = m_1 x_1 + \frac{1}{2}(m_0 - m_1)(|x_1 + 1| - |x_1 - 1|) \qquad (5)$$

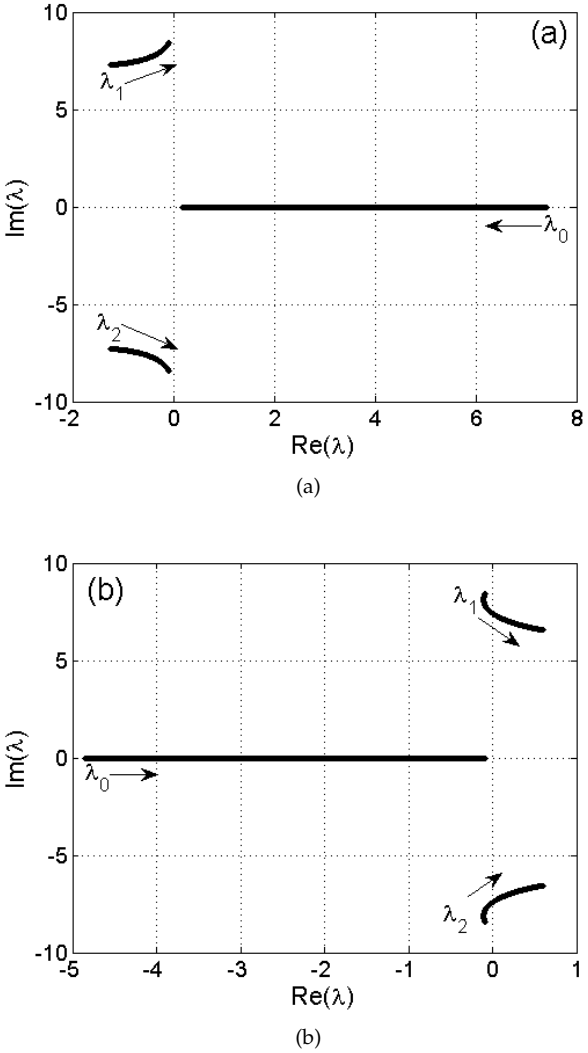

Figure 2 Eigenvalues locus (a) [(resp. (b) to the nontrivial equilibria $S_{1,2}$]obtained with $1 \leq \alpha \leq 38$ for $\beta = 73.04968$

Remarks that the parameter values used in this works are the one of the model call C-12 studied in Tsuneda (2005). It is obvious that, Chua's circuit is among the simplest circuit reported to date capable to plethora of nonlinear behaviors. In contrast to the work done by Kengne in 2017 Kengne (2017) were the nonlinear element has been implemented with a smooth nonlinearity $f(x) = ax^3 + bx$, we considered Chua's equation based on its original nonlinearity with piecewise-linear function as define in Eq.5. The aim of this consideration is to show that the original Chua's model without any modification can display the simultaneous existence of up to four disconnected attractors for the same set of the circuit parameters which has never been highlighted in the previous works focused on the dynamics of this original model.

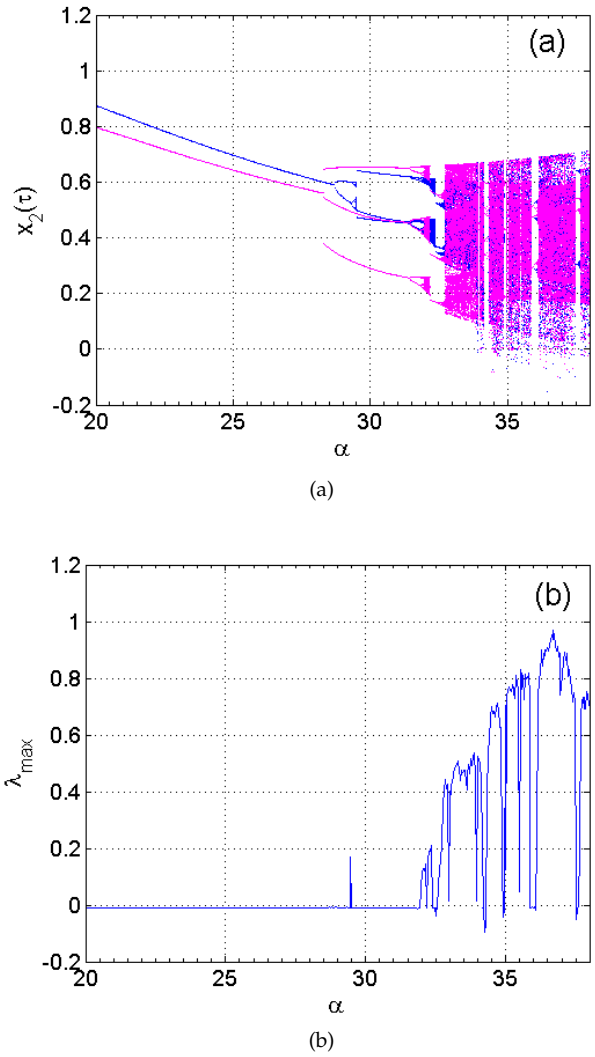

Figure 3 Bifurcation diagram (a) and the corresponding graph (b) of largest LE ($\lambda_{\max}$).

Stationary point analysis

In the investigation on the nonlinear dynamic systems, stationary points possess a key role. This role is justified by the fact that they enable to determine whether the attractors generated are self-excited when the stationary points are unstable or whether the attractors generated are hidden Pham *et al.* (2019). Hidden attractors are associated to systems with the following properties: systems without equilibria Jafari *et al.* (2013); Njitacke *et al.* (2017), systems with stable equilibria Wang and Chen (2012) and systems having an uncountable number of equilibria (line, circular, elliptic, square ...) Gotthans and Petržela (2015); Gotthans *et al.* (2016); Njitacke *et al.* (2018). The stationary points of the considered Chua's circuit are obtained by checking the solutions of the following equation.

$$\begin{cases} k\alpha\left(x_2 - x_1 - f\left(x_1\right)\right) = 0 \\ k\left[x_1 - x_2 + x_3\right] = 0 \\ k\left(-\beta x_2 - \gamma x_3\right) = 0 \end{cases} \tag{6}$$

The breakpoints are located at $x_1 = 1$ and $x_1 = -1$ therefore, $f\left(x_1\right)$ can be rewritten

$$f\left(x_1\right) = \begin{cases} m_1 x_1 + \left(m_0 - m_1\right) & x_1 > +1 \\ m_0 x_1 \quad -1 \geq x_1 \leq +1 \\ m_1 x_1 - \left(m_0 - m_1\right) & x_1 < -1 \end{cases} \tag{7}$$

Then, the three stationary points of the model can know be express as

$S_0 = \begin{pmatrix} 0, & 0, & 0 \end{pmatrix}$ and $S_{1,2} = \begin{pmatrix} \pm\bar{x}_1 & \frac{\pm\bar{x}_1\gamma}{\gamma+\beta} & \frac{\mp\bar{x}_1\beta}{\gamma+\beta} \end{pmatrix}$ in which $\bar{x}_1$ is given by $\bar{x}_1 = \frac{m_0 - m_1}{\frac{\gamma}{\gamma+\beta} - 1 - m_1}$

It is clear that $S_{1,2}$ are symmetric compared to the origin therefore they can share an identical stability ownership. This symmetry stability is also associated to the fact that the model remains unchanged under the permutation $(x_1, x_2, x_3) \Leftrightarrow (-x_1, -x_2, -x_3)$. Consequently (x_1, x_2, x_3) and $(-x_1, -x_2, -x_3)$ share a pair of solution for the same range of the system parameters. This symmetric ownership can enable us to predict the finding of the coexisting attractor that we want to highlight in the model studied (see Fig.5).

The stability of the model around any rest point $(\bar{x}_1, \bar{x}_2, \bar{x}_3)$ is analyzed by computing the Jacobian matrix of the Chua's model with piecewise-linear function given in Eq. 8.

Based on this Jacobian matrix, the eigenvalues which are tied to it are determined by solving the characteristic equation as depicted in Eq.(9)

$$\det\left(\lambda I - J\right) = \lambda^3 + a_1\lambda^2 + a_2\lambda + a_3 = 0 \tag{9}$$

Considering the assumptions of the Routh–Hurwitz criterion, and knowing that the polynomial coefficients of the Eq. (9) are all nonzero, the obligatory and adequate cases for the real parts of the roots of Eq. (9) to be positive are:

$$\begin{aligned} a_1 &> 0 \\ a_1 a_2 - a_3 &> 0 \\ a_3 &> 0 \end{aligned} \tag{11}$$

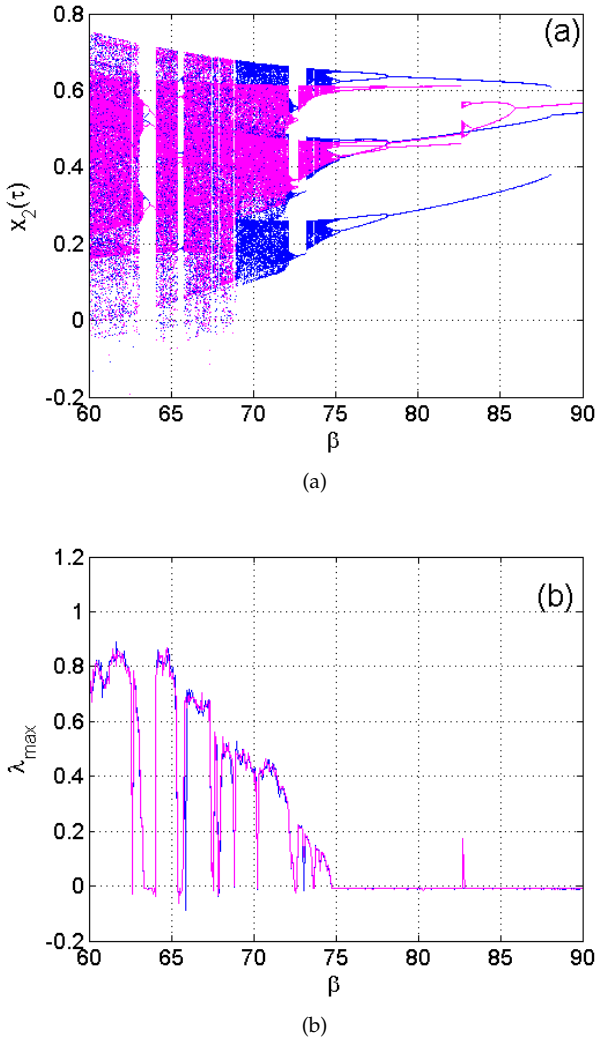

Figure 4 Bifurcation diagram (a) and the corresponding graph (b) of largest LE ($\lambda_{\max}$).

$$M_j = \begin{bmatrix} k\alpha\left(-1-\left(m_1+0.5\left(m_0-m_1\right)\left(sign\left(\bar{x}_1+1\right)-sign\left(\bar{x}_1-1\right)\right)\right)\right) & k\alpha & 0 \\ k & -k & k \\ 0 & -k\beta & -k\gamma \end{bmatrix} \tag{8}$$

$$\begin{cases} a_1 = \left(2489\alpha\right)/25000 + \left(12213\alpha sign\left(\bar{x}_1-1\right)\right)/100000 - \left(12213\alpha sign\left(\bar{x}_1+1\right)\right)/100000 + 403/2500 \\ a_2 = \beta - \left(61496933\alpha\right)/62500000 + \left(4921839\alpha sign\left(\bar{x}_1-1\right)\right)/250000000 - \left(4921839\alpha sign\left(\bar{x}_1+1\right)\right)/250000000 \\ \quad - 2903/2500 \\ a_3 = \left(35454339\alpha sign\left(\bar{x}_1+1\right)\right)/250000000 - \left(35454339\alpha sign\left(\bar{x}_1-1\right)\right)/250000000 - \left(79800567\alpha\right)/62500000 \\ \quad + \left(2489\alpha\beta\right)/25000 + \left(12213\alpha\beta sign\left(\bar{x}_1-1\right)\right)/100000 - \left(12213\alpha\beta sign\left(\bar{x}_1+1\right)\right)/100000 \end{cases} \tag{10}$$

Since that α is not related to the value of any rest point, it's then important to evaluate the global stability of the model by plotting the eigenvalues locus in terms of stationary point S_0 respectively $S_{1,2}$ (see Fig.2) when the bifurcation parameter α is sweep in the range $1 \leq \alpha \leq 38$. According to the graph shown in Fig.2, it can be observed that, the origin S_0, has eigenvalues with one positive real root. For the nontrivial stationary point $S_{1,2}$ possess eigenvalues with one negative real root. Thus, from this analysis of the eigenvalues associated to the model of Chua's oscillator under consideration, the model is always unstable and displays self-excited dynamics Negou and Kengne (2018); Njitacke *et al.* (2019); Pham *et al.* (2016); Tagne *et al.* (2019).

NUMERICAL INVESTIGATION

In this section, the analyses tools are simulated under a work space equipped with Intel i7-2450M, 16GB RAM where we run both MATLAB and Turbo Pascal softwares. We exploit usual nonlinear analysis tools to find the various windows of the parameters space for which the Chua's model with piecewise-linear function exhibits hysteretic dynamics. For this work, a fixed time step of $\Delta t = 0.002$ is used. During our investigations very long time is used to allow the transient behavior to be suppressed. Graph of Lyapunov exponent associated to each bifurcation diagram are computed using the Wolf et al. Wolf *et al.* (1985) algorithm.

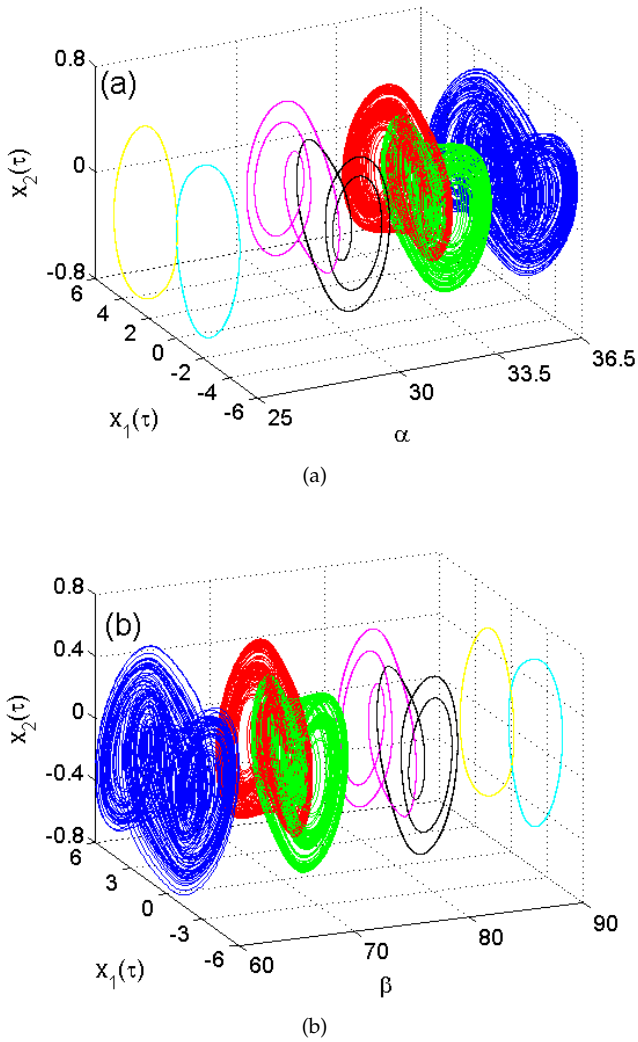

Figure 5 Three dimensional projections of the attractors in the (α, x_1, x_2) and (β, x_1, x_2) axes showing symmetry property of the model and route to chaos in (a) as depicted in Fig.3 and (b) as depicted in Fig.4. Initial conditions are $(\pm 1, 0, 0)$.

Dynamics with coexisting Bifurcations

Coexistence of bifurcations has been already found in several variant of Chua's oscillator Bao *et al.* (2016, 2015a); Pham *et al.* (2019). Recently this phenomenon of coexisting bifurcation has been reported in the Chua's oscillator having a smooth cubic nonlinearity but not yet in the original Chua's oscillator exploiting piecewise-linear function as nonlinearity. Fig.3 (a) shows a bifurcation diagram computed using the technique describes above. This method enables to increase respectively decrease the control parameter α.

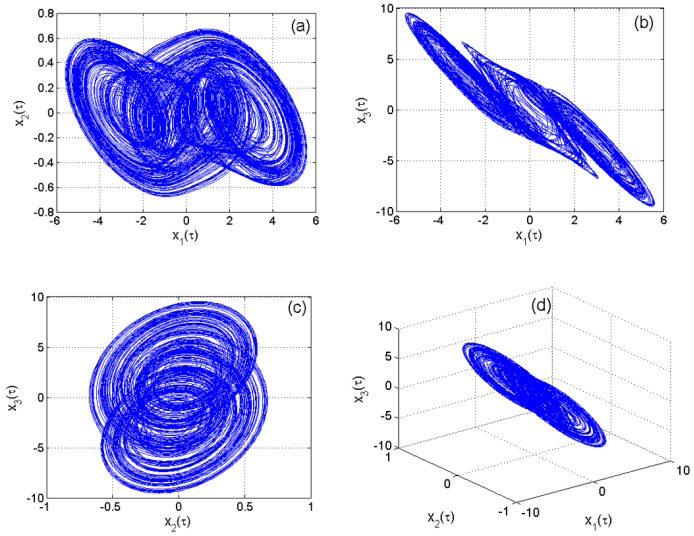

Figure 6 The phase portraits for $\alpha = 35$ in initial conditions $(-0.2, -0.002, 0.1)$.

In each case, the end state at each variation of the control parameter α is used as the initial state for the next iteration. When sweeping α in the windows $20 \leq \alpha \leq 38$ two sets of data are superposed. The one in blue is obtained by sweeping up the bifurcation parameter while de one in magenta in captured by sweeping down the bifurcation parameter as shown in Fig.3 (a). Fig.3 (b) displays the graph of maximum Lyapunov exponent corresponding to the blue diagram depicted in (a). From these two separated diagrams (blue and magenta), hysteretic dynamics can be easily explained using the discrepancy between both diagrams. From Fig.3 and Fig.4, it can be observed that, when sweeping either α or β Chua's circuit with piecewise-linear function displays plethora of behaviors.

In Fig.5 we have several 3D projection of the attractors which appear in symmetric pair in order to restore the exact symmetric of the model. When increasing the parameter α (four discrete values) the dynamics of the system varies from a pair of periodic attractor and end with a symmetric chaotic attractor. In contrast when varying β (four discrete values) the dynamics of the system varies form a symmetric chaotic attractor. For a specific value of the bifurcation parameter $\alpha = 35$ selected in Fig. 3; the model exhibits double scroll chaotic orbit. Fig.6 shows in (a-c) the 2D projection of the chaotic orbit in various plane as well as it corresponding 3D

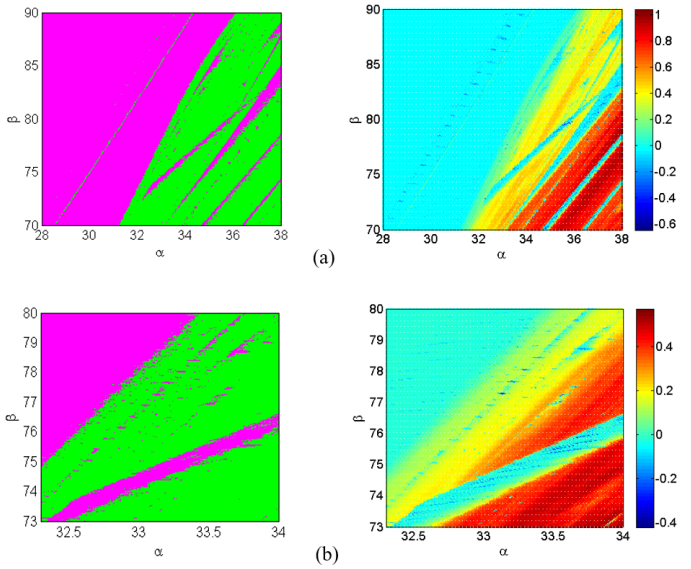

Figure 7 Two parameter diagram (left) and lyapunov stability diagram (right).

projection in the last quadrant. Finally, the two parameter diagram (left) and the maximal Lyapunov exponent (right) are displayed in Fig.7. On the two diagrams, the set of parameters which provide periodic oscillations are painted in magenta while the one providing chaotic oscillations are painted in green. Remark that, if other of theses diagrams is computed starting from initial states which are different from $(-0.2, -0.002, 0.1)$ (the one used to compute Fig.7) the results may be different because of the hysteresis dynamics of the investigated model.

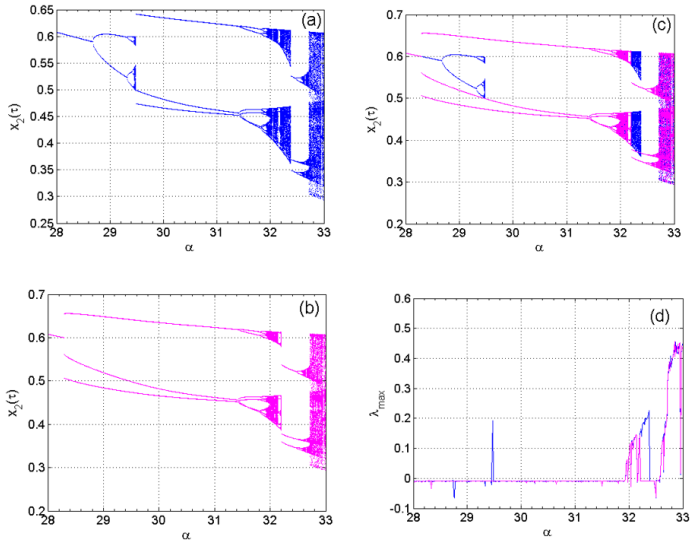

Figure 8 Two data sets corresponding to the incremental (a) and decreasing (b) values of the bifurcation control parameters respectively are provided and superimposed in (c). (d) the corresponding graph of largest LE of each diagram in (c).

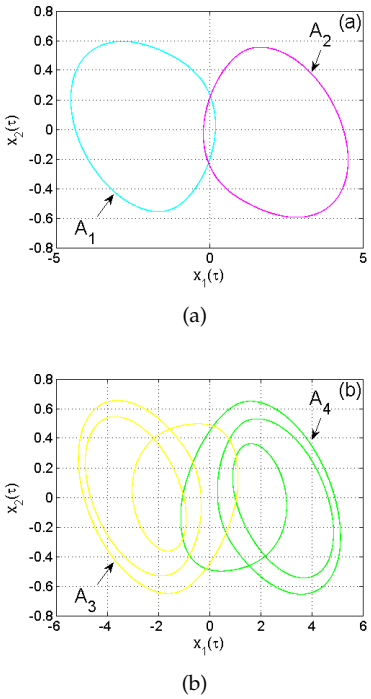

Figure 9 Superposition of four coexisting different periodic orbits for $\alpha = 28.5$. Initial conditions $(x_1(0), x_2(0), x_3(0))$ are $(\pm 1.2, 0, 0)$ and $(\pm 0.8, 0, 0)$ respectively.

Multistability and basins of initial conditions

The simultaneous existence (coexistence) of attractors in an oscillator sharing the same set of system parameters. Some extreme manifestations of such behavior generally conduct to extreme multistability Bao *et al.* (2016) or mega-stability Leutcho *et al.* (2020,?); Sprott *et al.* (2017); Tuna *et al.* (2019). In such system bifurcations that can occur depend only on the variation on the initial conditions. Among some nonlinearities are found hybrid diode, active diodes, RC memristor with diode bridge, Flux control just to name a few Bao *et al.* (2016); Chen *et al.* (2015); Bao *et al.* (2016). Recently Kengne in 2017 Kengne (2017) highlight the simultaneous existence of up to four disconnected attractors in the Chua's oscillator a smooth nonlinearity $f(x) = ax^3 + bx$. Although some immense works already done on Chua's oscillator, no work has ever report this widespread in the original Chua's circuit with PWL function as nonlinearity thus, merit to be investigated.

Fig.8 displays an extension of the diagram of Fig.3. A window of coexisting bifurcations which support the hysteretic dynamics are observed. For example when $\alpha = 28.5$, the Chua's circuit displays the simultaneous existence of two pair of periodic attractors including a pair period-1 limit cycle and a pair of period-3 limit cycle, using different initial states in Fig.9.

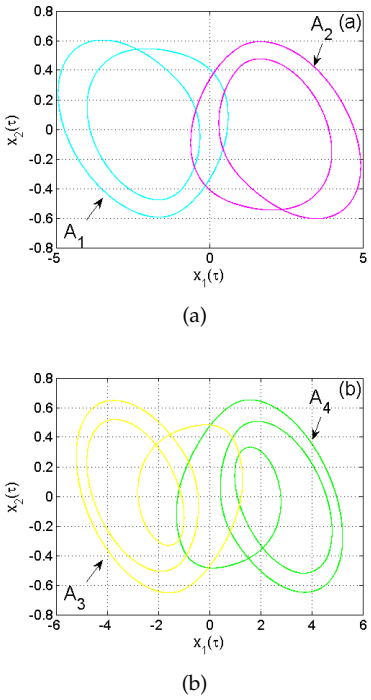

Figure 10 Superposition of four coexisting different periodic orbits for $\alpha = 29$. Initial conditions $(x_1(0), x_2(0), x_3(0))$ are $(\pm 0.8, 0, 0)$ and $(\pm 1.2, 0, 0)$ respectively.

For $\alpha = 29$ the Chua's circuit displays the simultaneous existence of two pair of periodic attractors including some limit cycles with different initial states in Fig.10. When further increase the control parameter to $\alpha = 29.47$ rep. $\alpha = 32.3$ the model exhibits the simultaneous existence four different orbits among which a pair of chaotic orbits and of a pair of period-3 limit cycle for different initial states as presented in Fig.11 resp. in Fig.12.

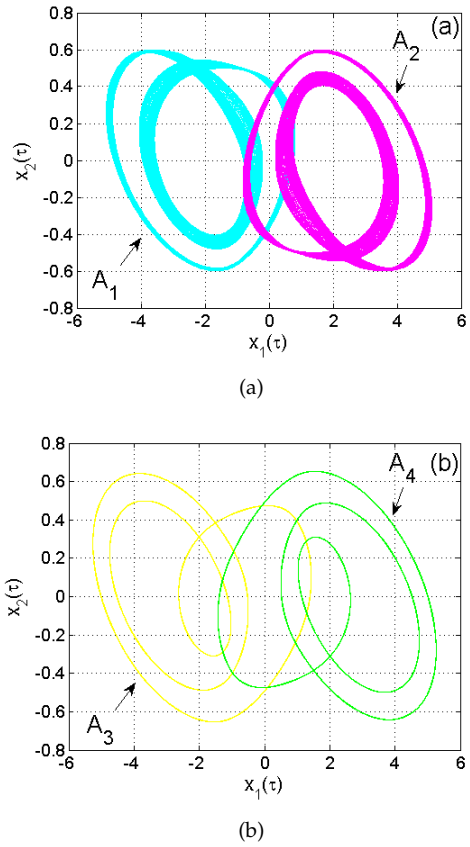

Figure 11 Superposition of four coexisting different periodic orbits including a pair of chaotic orbits as well as a periodic one for $\alpha = 29.47$. Initial conditions $(x_1(0), x_2(0), x_3(0))$ are $(\pm 1.44, 0, 0)$ and $(\pm 1.2, 0, 0)$ respectively.

This simultaneous existence of periodic and chaotic orbits discovered in this works can be viewed as another contribution for the repertory of behavior already found during the previous investigation of this original Chua's circuit with piecewise-linear function. In the case Fig.12 we have computed the eigenvalues associated to each stationary point. It is found that, the eigenvalues related to origin S_0 are $\lambda_0 = 6.8313$ and $\lambda_{1,2} = -1.1593 \pm 7.3028$i while the one related to the non-trivial fixed point $S_{12} = (\pm 2.93, \mp 0.0473, \mp 2.9773)$ are $\lambda_0 = -4.3618$ and $\lambda_{1,2} = 0.4924 \pm 6.6453$i.

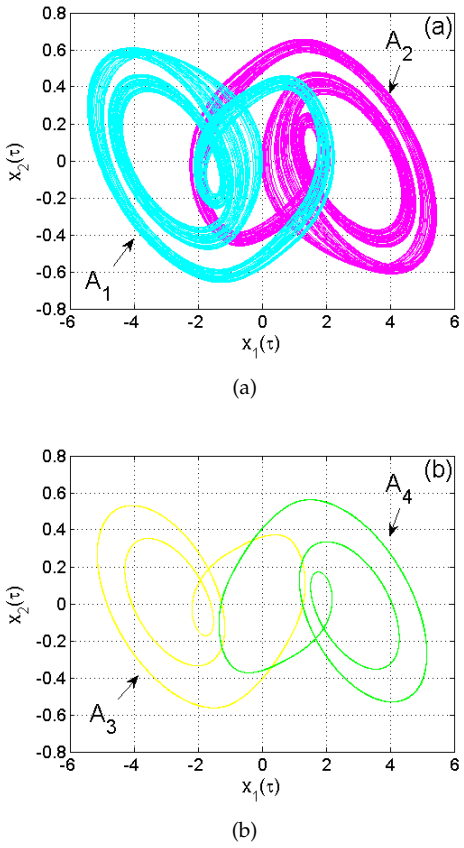

Figure 12 Superposition of four coexisting different periodic orbits including a pair of chaotic orbits as well as a periodic one for $\alpha = 32.3$. Initial conditions $(x_1(0), x_2(0), x_3(0))$ are $(\pm 1.44, 0, 0)$ and $(\pm 1.52, 0, 0)$ respectively.

The obtained eigenvalues are in good agreement with the one plotted in Fig.2 and yield the conclusion that coexisting attractors found in this work are self-existed instead of hidden Njitacke *et al.* (2019); Pham *et al.* (2016, 2019); Tagne *et al.* (2019). For each coexisting attractors captured in Fig.12, Fig.13 represents cross sections of basin of attraction associated to each attractor. From Fig.13 it can be observed that each attractor has its set of initial conditions which intercepts with the one of its direct neighbor.

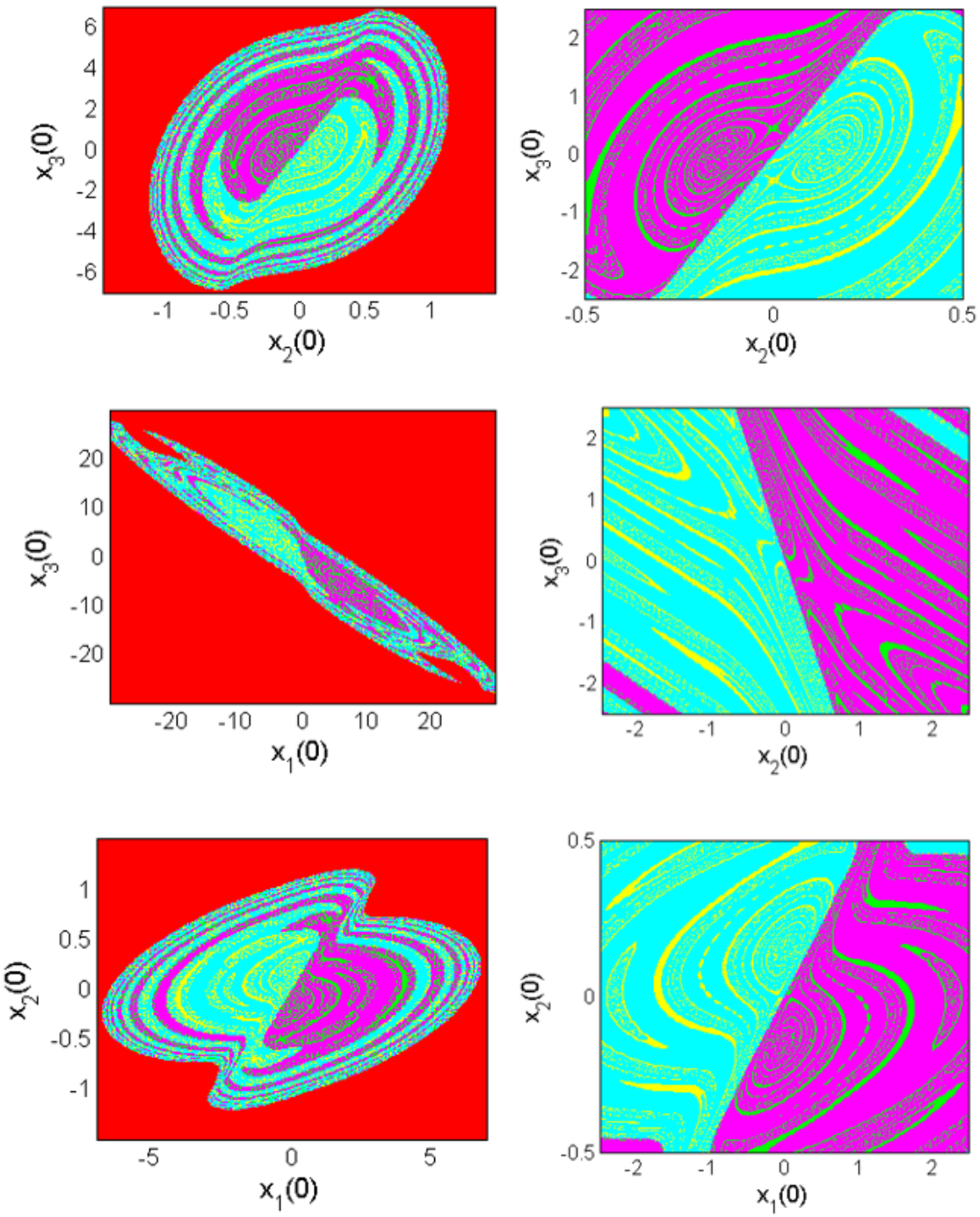

Figure 13 Basin of attraction domain for$x_1(0) = 0$, $x_2(0) = 0$ and $x_3(0) = 0$.

ANNIHILATION OF THE MULTISTABILITY IN THE CHUA'S OSCILLATOR BASED ON LINEAR AUGMENTATION SCHEME

Presentation of the control method

From the theory Sharma *et al.* (2011) the linear augmentation control scheme enables a coupling between a nonlinear system and linear system as following:

$$\begin{cases} \dot{X} = F(X) - \delta U \\ \dot{U} = -\eta U - \delta (X - E) \end{cases} \tag{12}$$

Here, $\dot{X} = F(X)$ represents any autonomous nonlinear dynamical system, X the m-dimensional state vector of the uncontrolled system. The parameter δ defines the intensity of interaction between the two structures. The vector U relates the dynamics of the linear system $\dot{U} = -\eta U$. Parameter E plays the key role of targeting desired attractor from the augmented system Fonzin Fozin *et al.* (2019); Fozin *et al.* (2019); Sharma *et al.* (2013, 2015). Henceforth, appropriate selection of parameter E close to any of the unstable steady state leads to the disappearance of some coexisting attractors. It is worth to underline that a unique targeted attractor is obtained for higher values of the coupling strength and thus turns the multistable system to a mono-stable one.

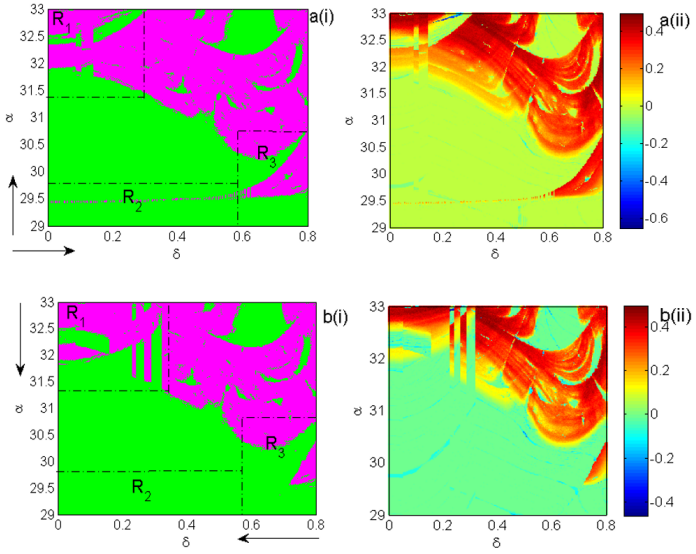

Figure 14 Two parameter diagram (left) and lyapunov stability diagram (right).

Let now apply the linear augmentation scheme to the Chua's system with PWL nonlinearity. The controller is applied along the x_2 variable with the coupling strength δ as shown in Eq.(13).

$$\begin{cases} \frac{dx_1}{dt} = k\alpha \left(x_2 - x_1 - m_1 x_1 + \frac{1}{2}(m_0 - m_1)(|x_1 + 1| - |x_1 - 1|) \right) \\ \frac{dx_2}{dt} = k(x_1 - x_2 + x_3) + \delta u \\ \frac{dx_3}{dt} = k(-\beta x_2 - \gamma x_3) \\ \frac{du}{dt} = -\eta u - \delta (x_2 - e) \end{cases} \tag{13}$$

It is worthy to recall that the choice of scalar coupling is mostly justified by both engineering requirements (i.e., optimization of resources and great flexibility in the design of communication systems) and recent results of control and synchronization on chaotic systems Lian *et al.* (2002); Peng *et al.* (1996). Indeed, vector coupling implies higher energy and resources consumption than scalar coupling.

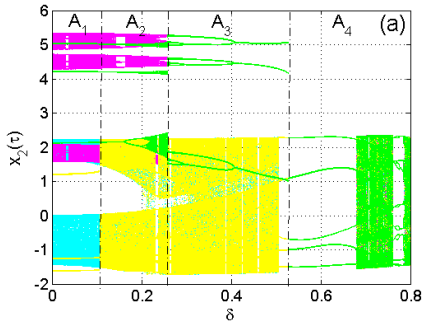

(a)

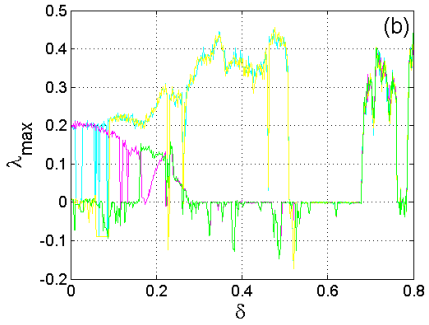

(b)

Figure 15 Bifurcation diagram (a) and corresponding graph of maximum LEs.

Control of multistability in Chua's oscillator

Results of this control method are provided in Fig.14 using the Two-parameter diagram and corresponding graph of the Lyapunov stability exponent in the parameter space (δ, α). The computation method used here is the same like the one exploited in the previous section. Green color justifies periodic oscillations while the magenta color justifies chaotic motions. A good accordance is observed between Two-parameter diagrams (left) and corresponding maximal Lyapunov exponent diagrams (right). The diagrams are obtained by sweeping up (Fig.14 (a)) and down (Fig.14 (b)) the bifurcation parameter of the uncontrolled Chua's circuit and coupling strength simultaneously. Globally, from these diagrams three parameters space namely (R1), (R2) and (R3) can be observed. The regions correspond to the set of parameter for with the model displays hysteretic dynamics which gives birth to the phenomenon of coexistence of multiple stable states.

When weeping up the control parameter δ in the range $[0 \rightarrow 0.8]$ as it can be seen in Fig.15, four set of data are superimposed in the bifurcation diagram as well as its corresponding graph of maximum Lyapunov exponent. Each set of data (marked by cyan, green, magenta and yellow colors) corresponds to the route follows by each attractor during the control mechanism. As depicted in Fig.15 three crises enable all the plotted routes to merge along the one in red as for higher values of the coupling strength. In the region (A1) of Fig.13 and for very small values of δ (i.e., $\delta \approx 0.1$), four attractors coexist including two chaotic attractors (cyan color and magenta color) with two periodic attractors (yellow color and green color).

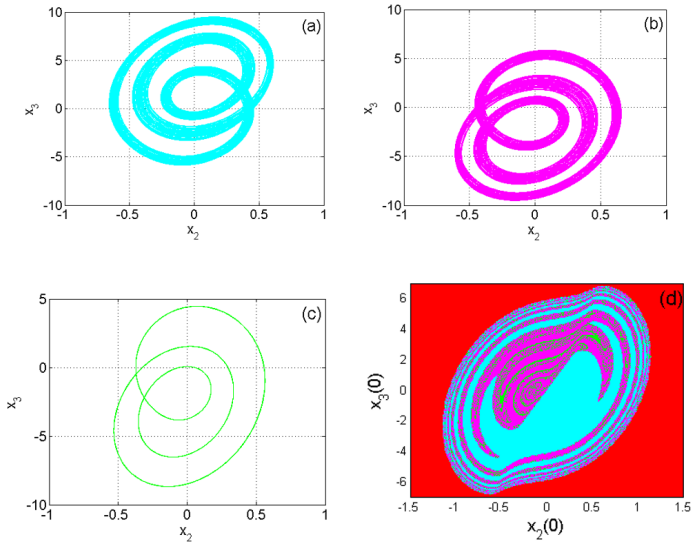

Figure 16 Coexistence of a pair of asymmetric chaotic attractor ((a) and (b)) with asymmetric periodic three ((c)) showing multistability phenomenon with the Basin of attraction (d) in the plane $(x_2(0), x_3(0))$ when $\delta = 0.128$.

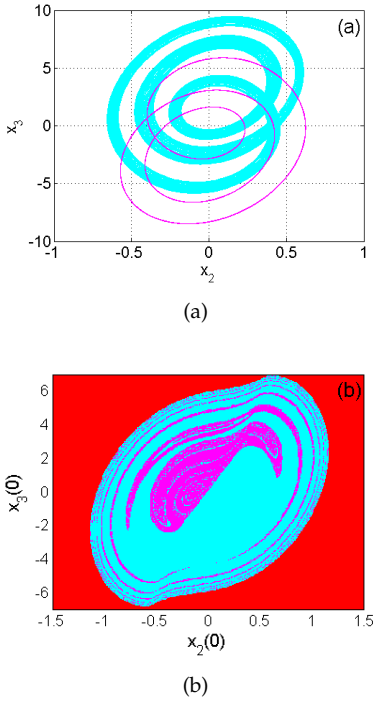

Figure 17 Coexistence of an asymmetric chaotic attractor (a) with asymmetric periodic three showing multistability phenomenon with the basin of attraction (b) in the plane $(x_2(0), x_3(0))$ when $\delta = 0.49$.

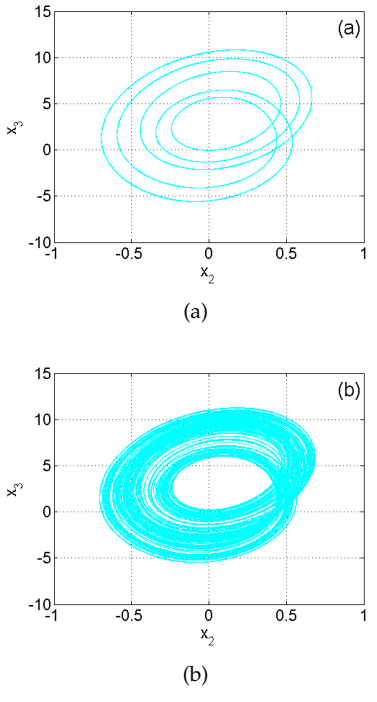

Figure 18 Period-5 attractor (a) and asymmetric chaotic attractor (b) showing various surveying attractor obtained after the control gaol when $\delta = 0.6$ and $\delta = 0.7$ respectively.

At the upper boundary of (A1) the diagram in yellow (periodic one) undergoes a crisis (first crisis) and merges with the diagram in cyan. In the region (A2), because of the previous merging crisis, there are only three distinct diagrams whose follow their bifurcations (see region A2). For a discrete value $\delta = 0.128$ we have the coexistence of three disconnected attractors, involving a period-3 limit cycle with a pair of chaos as presented in Fig.16. The demarcation region of each coexisting attractor in region A2 is provided in Fig.16d. At the upper boundary of (A2) a crisis (second crisis) enables the diagram in green displaying chaotic dynamics to merge with the diagram in magenta. In the region (A3), we observe the superposition of two diagrams including a periodic and chaotic one. In this region for a discrete value $\delta = 0.49$, the Chua's oscillator displays coexistence of a period-3 limit cycle with an asymmetric chaotic attractor (see Fig.17).

The basin of attraction associated to each coexisting attractor is computed and plotted in Fig.15b. At the upper boundary of (A3) a crisis (third crisis) enables the diagram in magenta displaying period-3 limit cycle to merge with the diagram in cyan. In the region (A4), when the critical value $\delta = 0.52$ all the diagrams have already merge with the cyan one and the control goal is achieved as depicted in region (A4). For $\delta = 0.6$ (resp. $\delta = 0.7$) Fig.18a (resp. Fig.18b) displays the unique periodic (resp. chaotic) attractors which have survived through the control scheme. We can say that, the route exhibited by the cyan diagram is a magnetized route which attracts towards it all the others route as the control parameter is increased. Also, It is worth to emphasize here that the result of multistability control on the Chua's system with PWL nonlinearity obtained in this work has never been presented before and thus merit to be shared.

CONCLUSION

In the present work, we have addressed the suppression of multistability in the original Chua's circuit with the traditional piecewise-linear nonlinearity. Using usual nonlinear bifurcation diagrams windows of coexisting dynamics of the model have been investigated. The main result of this paper is the output of different windows in the parameter space where the Chua's circuit with a piecewise-linear nonlinearity displays the phenomenon of the simultaneous existence of multiple coexisting orbits, including coexistence of four disjointed oscillatory periodic and chaotic orbits depending only on initial conditions for a large range of circuit parameters values. The linear augmentation method has been also applied on the model to control the four coexisting orbits obtained from hysteretic investigation. Then the pair of periodic orbits which were coexisting with the pair of chaotic orbits have been suppressed and only a unique orbit remains. Since the Chua's model investigated in this work processes three equilibrium points and displays the coexistence of four attractors, the control of the coexisting attractors with selection of chaotic attractor based on equilibria and its electronics implementation as well as its application to image encryption would deserve the topic of our future work.

Conflicts of interest

The authors declare that there is no conflict of interest regarding the publication of this paper.

LITERATURE CITED

Adiyaman, Y., S. Emiroglu, M. K. Ucar, and M. Yildiz, 2020 Dynamical analysis, electronic circuit design and control application of a different chaotic system. Chaos Theory and Applications **2**: 10–16.

Bao, B., F. Hu, M. Chen, Q. Xu, and Y. Yu, 2015a Self-excited and hidden attractors found simultaneously in a modified chua's circuit. International Journal of Bifurcation and Chaos **25**: 1550075.

Bao, B., P. Jiang, H. Wu, and F. Hu, 2015b Complex transient dynamics in periodically forced memristive chua's circuit. Nonlinear Dynamics **79**: 2333–2343.

Bao, B.-C., Q. Xu, H. Bao, and M. Chen, 2016 Extreme multistability in a memristive circuit. Electronics Letters **52**: 1008–1010.

Chen, M., J. Yu, and B.-C. Bao, 2015 Finding hidden attractors in improved memristor-based chua's circuit. Electronics Letters **51**: 462–464.

Chua, L., M. Komuro, and T. Matsumoto, 1986 The double scroll family. IEEE transactions on circuits and systems **33**: 1072–1118.

Chua, L. O., 1994 Chua's circuit 10 years later. International Journal of Circuit Theory and Applications **22**: 279–305.

Chua, L. O., 1998 *CNN: A paradigm for complexity*, volume 31. World Scientific.

Duan, Z., J. Wang, R. Li, and L. Huang, 2007 A generalization of smooth chua's equations under lagrange stability. International Journal of Bifurcation and Chaos **17**: 3047–3059.

Fonzin Fozin, T., R. Kengne, J. Kengne, K. Srinivasan, M. Souffo Tagueu, *et al.*, 2019 Control of multistability in a self-excited memristive hyperchaotic oscillator. International Journal of Bifurcation and Chaos **29**: 1950119.

Fozin, T. F., G. Leutcho, A. T. Kouanou, G. Tanekou, R. Kengne, *et al.*, 2019 Multistability control of hysteresis and parallel bifurcation branches through a linear augmentation scheme. Zeitschrift für Naturforschung A **75**: 11–21.

Gotthans, T. and J. Petržela, 2015 New class of chaotic systems with circular equilibrium. Nonlinear Dynamics **81**: 1143–1149.

Gotthans, T., J. C. Sprott, and J. Petrzela, 2016 Simple chaotic flow with circle and square equilibrium. International Journal of Bifurcation and Chaos **26**: 1650137.

Hartley, T. T., 1989 The duffing double scroll. In *1989 American Control Conference*, pp. 419–424, IEEE.

Huang, A., L. Pivka, C. W. Wu, and M. Franz, 1996 Chua's equation with cubic nonlinearity. International Journal of Bifurcation and Chaos **6**: 2175–2222.

Jafari, S., J. Sprott, and S. M. R. H. Golpayegani, 2013 Elementary quadratic chaotic flows with no equilibria. Physics Letters A **377**: 699–702.

Kengne, J., 2017 On the dynamics of chua's oscillator with a smooth cubic nonlinearity: occurrence of multiple attractors. Nonlinear Dynamics **87**: 363–375.

Kengne, J., Z. N. Tabekoueng, and H. Fotsin, 2016 Coexistence of multiple attractors and crisis route to chaos in autonomous third order duffing–holmes type chaotic oscillators. Communications in Nonlinear Science and Numerical Simulation **36**: 29–44.

Kingni, S. T., C. Ainamon, V. K. Tamba, and J. C. OROU, 2020 Directly modulated semiconductor ring lasers: Chaos synchronization and applications to cryptography communications. Chaos Theory and Applications **2**: 31–39.

Leonov, G., N. Kuznetsov, and V. Vagaitsev, 2011 Localization of hidden chua's attractors. Physics Letters A **375**: 2230–2233.

Leutcho, G. D., S. Jafari, I. I. Hamarash, J. Kengne, Z. T. Njitacke, *et al.*, 2020 A new megastable nonlinear oscillator with infinite attractors. Chaos, Solitons & Fractals **134**: 109703.

Lian, K.-Y., P. Liu, T.-S. Chiang, and C.-S. Chiu, 2002 Adaptive synchronization design for chaotic systems via a scalar driving signal. IEEE Transactions on Circuits and Systems I: Fundamental Theory and Applications **49**: 17–27.

Matsumoto, T., 1984 A chaotic attractor from chua's circuit. IEEE Transactions on Circuits and Systems **31**: 1055–1058.

Negou, A. N. and J. Kengne, 2018 Dynamic analysis of a unique jerk system with a smoothly adjustable symmetry and nonlinearity: Reversals of period doubling, offset boosting and coexisting bifurcations. AEU-International Journal of Electronics and Communications **90**: 1–19.

Njitacke, Z., J. Kengne, T. F. Fozin, B. Leutcha, and H. Fotsin, 2019 Dynamical analysis of a novel 4-neurons based hopfield neural network: emergences of antimonotonicity and coexistence of multiple stable states. International Journal of Dynamics and Control **7**: 823–841.

Njitacke, Z., J. Kengne, and A. N. Negou, 2017 Dynamical analysis and electronic circuit realization of an equilibrium free 3d chaotic system with a large number of coexisting attractors. Optik **130**: 356–364.

Njitacke, Z., J. Kengne, R. W. Tapche, and F. Pelap, 2018 Uncertain destination dynamics of a novel memristive 4d autonomous system. Chaos, Solitons & Fractals **107**: 177–185.

Peng, J., E. Ding, M. Ding, and W. Yang, 1996 Synchronizing hyperchaos with a scalar transmitted signal. Physical Review Letters **76**: 904.

Pham, V.-T., S. Jafari, C. Volos, and L. Fortuna, 2019 Simulation and experimental implementation of a line–equilibrium system without linear term. Chaos, Solitons & Fractals **120**: 213–221.

Pham, V.-T., S. Jafari, X. Wang, and J. Ma, 2016 A chaotic system with different shapes of equilibria. International Journal of Bifurcation and Chaos **26**: 1650069.

Ramírez-Ávila, G. M. and J. A. Gallas, 2010 How similar is the performance of the cubic and the piecewise-linear circuits of chua? Physics Letters A **375**: 143–148.

Sharma, P. R., A. Sharma, M. D. Shrimali, and A. Prasad, 2011 Targeting fixed-point solutions in nonlinear oscillators through linear augmentation. Physical Review E **83**: 067201.

Sharma, P. R., M. D. Shrimali, A. Prasad, and U. Feudel, 2013 Controlling bistability by linear augmentation. Physics Letters A **377**: 2329–2332.

Sharma, P. R., M. D. Shrimali, A. Prasad, N. V. Kuznetsov, and G. A. Leonov, 2015 Controlling dynamics of hidden attractors. International Journal of Bifurcation and Chaos **25**: 1550061.

Sprott, J. C., S. Jafari, A. J. M. Khalaf, and T. Kapitaniak, 2017 Megastability: Coexistence of a countable infinity of nested attractors in a periodically-forced oscillator with spatially-periodic damping. The European Physical Journal Special Topics **226**: 1979–1985.

Tagne, R. M., J. Kengne, and A. N. Negou, 2019 Multistability and chaotic dynamics of a simple jerk system with a smoothly tuneable symmetry and nonlinearity. International Journal of Dynamics and Control **7**: 476–495.

Tsuneda, A., 2005 A gallery of attractors from smooth chua's equation. International Journal of Bifurcation and Chaos **15**: 1–49.

Tuna, M., A. Karthikeyan, K. Rajagopal, M. Alcin, and İ. Koyuncu, 2019 Hyperjerk multiscroll oscillators with megastability: Analysis, fpga implementation and a novel ann-ring-based true random number generator. AEU-International Journal of Electronics and Communications **112**: 152941.

Wang, X. and G. Chen, 2012 A chaotic system with only one stable equilibrium. Communications in Nonlinear Science and Numerical Simulation **17**: 1264–1272.

Wolf, A., J. B. Swift, H. L. Swinney, and J. A. Vastano, 1985 Determining lyapunov exponents from a time series. Physica D: Nonlinear Phenomena **16**: 285–317.

Xu, Q., Y. Lin, B. Bao, and M. Chen, 2016 Multiple attractors in a non-ideal active voltage-controlled memristor based chua's circuit. Chaos, Solitons & Fractals **83**: 186–200.

Zhong, G.-Q., 1994 Implementation of chua's circuit with a cubic nonlinearity. IEEE Transactions on Circuits and Systems I: Fundamental Theory and Applications **41**: 934–941.

Zhong, G.-Q. and F. Ayrom, 1985 Experimental confirmation of chaos from chua's circuit. International journal of circuit theory and applications **13**: 93–98.

How to cite this article: Njitacke, Z. T., Fozin, T. F., Kamdjeu, L. K., Leutcho, G. D., Kengne, E. M., and Kengne, J. Chaos Theory and its Application: Multistability and its Annihilation in the Chua's Oscillator with Piecewise-Linear Nonlinearity, 2(2), 77-89, 2020.